Biosensors and Bioelectronics ■ (■■■■) ■■■–■■■

Contents lists available at ScienceDirect

Biosensors and Bioelectronics

journal homepage: www.elsevier.com/locate/bios

Real-time monitoring of glucose and phenols intestinal absorption through an integrated Caco-2TC7cells/biosensors telemetric device: Hypoglycemic effect of fruit phytochemicals

Barberis Antonio [a,1], Garbetta Antonella [b,1], Cardinali Angela [b], Bazzu Gianfranco [c], D.'Antuono Isabella [b], Rocchitta Gaia [c], Fadda Angela [a], Linsalata Vito [b], D.'Hallewin Guy [a], Serra Pier Andrea [a,c,*], Minervini Fiorenza [b]

[a] Institute of Sciences of Food Production (ISPA), National Research Council (CNR), Traversa La Crucca, 3 Regione Baldinca, 07100 Li Punti, Sassari, Italy
[b] Institute of Sciences of Food Production (ISPA), National Research Council (CNR), Via G. Amendola 122/O, 70125 Bari, Italy
[c] Department of Clinical and Experimental Medicine, Section of Pharmacology, University of Sassari, V.le San Pietro 43/B, 07100 Sassari, Italy

ARTICLE INFO

Article history:
Received 15 June 2016
Received in revised form
22 July 2016
Accepted 2 August 2016

Keywords:
Postprandial hyperglycemia
Enzyme biosensor
Caco-2TC7 cells
Glucose
Polyphenols

ABSTRACT

An integrated device for real-time monitoring of glucose and phenols absorption, that consists of a sensors/biosensors system (SB) and a Caco-2TC7 human intestinal cell culture, is described in this study. The SB is composed of a glucose oxidase-based biosensor, a sentinel platinum sensor, a laccase/tyrosinase-based biosensor and a sentinel carbon sensor, all located in the basolateral compartment (BC) of a cell culture plate. Caco-2TC7 cells, differentiated on culture inserts, separated the apical compartment that simulates the intestinal lumen, from the BC which represented the bloodstream. The system recorded currents relative to glucose (1 mM) absorption, obtaining bioavailability values (5.1%) comparable to HPLC analysis (4.8%). Phloridzin and phloretin, specific phenolic inhibitors of SGLT1 and GLUT2 glucose transporters, reduced the glucose transport of almost 10 times. They were minimally absorbed in the BC with a bioavailability of 0.13% and 0.49% respectively. The hypoglycemic potential of blueberry and pomegranate juices was also studied. In particular, the amount of glucose absorbed through the Caco-2TC7 monolayer was 8‰ for pomegranate and 1.7‰ for blueberry, demonstrating the potential hypoglycemic effect of the juices. Polyphenols absorption was also monitored by the SB and an increase was recorded during the first 50 min in presence of both blueberry and pomegranate juices, then a constant decrease occurred. The proposed device has been developed as innovative tool for the dynamic monitoring of natural compounds effects on glucose absorption, in order to manage postprandial hyperglycemia.

1. Introduction

Type 2 diabetes mellitus (T2DM), a disease that currently affect hundreds of million people worldwide, is associated with increased coronary artery, cerebrovascular and peripheral vascular diseases, with up to 80% of deaths in people with this pathology caused by cardiovascular disease. Hyperglycemia and fluctuations in blood glucose lead to generation of reactive oxygen species (ROS), which is the root cause of the development of insulin resistance, pancreatic β-cells dysfunction, impaired glucose tolerance and, finally, of T2DM (Ceriello and Motz, 2004). The correct managing of postprandial hyperglycemia is important for prevention of micro and macrovascular complications in T2DM (Wright Jr. et al., 2006).

Natural foods-based diets, rich in bioactive compounds, such as polyphenols, are attractive strategies to limit the glucose intestinal absorption and a potential tool of glycemic control. Various dietary polyphenols and their metabolites differently influence the carbohydrate metabolism at many levels (Atkinson et al., 2005; Rechner et al., 2002): inhibition of carbohydrate digestion and glucose absorption in the intestine, stimulation of insulin secretion from the β-cells, modulation of glucose release from the liver, activation of insulin receptors and glucose uptake in the insulin-sensitive tissues are only some of the hypothesized mechanisms of action (Chu et al., 2011; Shihabudeen et al., 2011; Hanhineva et al., 2010; Chacon et al., 2009). Previous studies, using fruits and

* Corresponding author at: Department of Clinical and Experimental Medicine, Section of Pharmacology, University of Sassari, V.le San Pietro 43/B, 07100 Sassari, Italy. Tel.: +39 079 228558; fax: +39 079 228525.
E-mail address: paserra@uniss.it (S.P. Andrea).
[1] Equally contributed to this study.

http://dx.doi.org/10.1016/j.bios.2016.08.007
0956-5663/

vegetables, demonstrated that some polyphenols can attenuate intestinal glucose absorption by inhibition of active uptake via sodium-dependent glucose transporter 1 (SGLT1) and facilitated transport by sodium-independent transporter 2 (GLUT2)(Farrell et al., 2013; Manzano and Williamson, 2010). Fruits like blueberry or pomegranate are important source of phenols (Barberis et al., 2015; Fischer et al., 2011). Anthocyanins from blueberry had the potency to alleviate symptoms of hyperglycemia in diabetic C57b1/6J mice (Grace et al., 2009), while an inhibition of the α-glucosidase activity was correlated with anthocyanins, total phenolic content and antioxidant activity of extracts of some pomegranate varieties (Kaur et al., 2014), strawberry and raspberry fruits (McDougall and Stewart, 2005).

Caco-2 intestinal cell model was widely used for the assessment of bioaccessibility, intestinal uptake and bioavailability of bioactive compounds (D'Antuono et al., 2015; Failla et al., 2014). Moreover, the model was also applied to investigate the attenuation of [^{14}C]-glucose transport by polyphenols (Farrell et al., 2013; Manzano and Williamson, 2010) for the high levels of cellular expression of the facilitated glucose transport proteins (GLUT 1 and 2) and SGLT1 (Johnston et al., 2005).

Biosensors are reliable tools to detect both glucose for clinical practice (Yoo and Lee, 2010) and phenols compounds (Rodríguez-Delgado et al., 2015). Glucose enzyme electrodes based on detection of hydrogen peroxide (H_2O_2) are known since 1962 (Clark and Lyons, 1962) and have been significantly improved during the last years. A simple and inexpensive telemetry device for the detection of extracellular brain glucose was implanted in the striatum of freely moving rats (Rocchitta et al., 2013). The glucose oxidase, being an oxidoreductase exhibiting a high β-D-glucose specificity and stability, is well-suited for applications in diabetes care (Arango Gutierrez et al., 2013). A bioelectrode based on glucose oxidase-nanoporous gold co-catalysis was developed for glucose monitoring in human serum (Wu et al., 2015). Concerning the detection of phenol compounds, a biomimetic biosensor based on lipidic layers containing tyrosinase and lutetium bisphthalocyanine was used (Apetrei et al., 2011). In addition, a tyrosinase-based biosensor (Carralero Sanz et al., 2005) and a laccase-based biosensor (Gomes et al., 2004) were both developed for polyphenols detection in wines.

In this paper, we combined a Caco-2TC7 intestinal model with a biosensors system to simulate, without radiolabeled compounds, physiological conditions of small intestine tract. The intestinal cellular model is an important tool to investigate the intestinal absorption (Artursson et al., 2012) and metabolism for the presence of the phase II enzymes (Teng et al., 2012). We propose a prototype of a diagnostic device, based on glucose oxidase (GOx) biosensors and on laccase/tyrosinase (Lac/Tyr) biosensors, for the real-time telemetric monitoring of glucose and phenols absorption by Caco-2TC7 human intestinal cell culture. The device was conceived for the on-line measurement of glucose intestinal absorption, in the absence and in the presence of hypoglycemic phytochemicals. The object was to realize a smart and safe tool to study the *in vitro* effects of phytochemicals on glucose absorption that could be useful for future studies on the managing of postprandial hyperglycemia with natural compounds.

2. Materials and methods

2.1. Reagents

The list of reagents used in this work and the methodologies for the solutions' preparation are reported in Supplementary data (S1.1 and S1.2).

2.2. Fruit samples, juice preparation and chemical composition analyses

Pomegranate fruits (*Punicagranatum* L.) *cv* Wonderful and blueberry fruits (*Vaccinumcorimbosum* L.) *cv* Brigitta blue were bought on the local market. Fruits were squeezed and the juices were filtered, centrifuged at 4629*g* for 10 min at 4 °C (centrifuge A. L.C.-4227R, A.L.C. s.r.l. Milano, Italy), stored in ultra-freezer at −80 °C and lyophilized. All freeze-dried samples were fully rehydrated for chemical composition analyses and *in vitro* assays. The pomegranate and blueberry juices were filtered with regenerated cellulose 45 μm (filter, diluted and analyzed for sugars content by HPLC-PAD system (Supplementary data S2.1) and for phenolic composition by HPLC-DAD analysis (Supplementary data S2.2 and S2.3).

2.3. Description of the diagnostic device

A Corning® 6-wells cell culture plate was modified (Fig. 1A) to be integrated with two potentiostats, twelve current-to-voltage converters that made up two sensor/biosensor systems (SBs): SB1 for glucose and SB2 for polyphenols detection.

The device was conceived to assess the glucose and polyphenols bioavailability by monitoring their transport from apical (which simulated the intestinal lumen) to basolateral compartment (which simulated the bloodstream) through a Caco-2TC7 cells monolayer (Fig. 1C). The electronics developed for this study was based on previous single-supply-powered designs (Barberis et al., 2014; Rocchitta et al., 2007; Serra et al., 2007). Both potentiostatic circuits (Fig. 2, P1 and P2) maintained the reference and auxiliary electrodes to the same fixed potential. Glucose biosensors (and the corresponding sentinels) were polarized at +700 mV *vs* Ag/AgCl pseudo-references and worked in oxidation mode for glucose transport assessment. Polyphenols biosensors (and the corresponding sentinels) were polarized at −100 mV *vs* Ag/AgCl pseudo-references and worked in reduction mode for polyphenols absorption estimation. The recorded data were acquired second-by-second, by an Arduino Due© embedded system averaged and transmitted by Bluetooth™ to a notebook every 5 s. A detailed description of the telemetry device is provided in Supplementary data (S3).

2.3.1. Basolateral compartment modification

Each potentiostat (Fig. 2) was connected with a Pt shared auxiliary electrode and a shared pseudo-reference electrode (Ag/AgCl) arranged at the bottom of the plate (Fig. 1D). Two lateral access holes for the working electrodes (WEs) of SB1 and SB2 were also provided for each well (Fig. 1B). The WEs were aligned in the free space between the bottom of the well and the bottom of the insert (Fig. 1C). Three wells of the plate were devoted to glucose detection and three to polyphenols detection. In the wells devoted to glucose detection, one hole was for a GOx-based biosensor and the other for a platinum sentinel sensor. In the wells devoted to polyphenols detection one hole was for a Lac/Tyr-based biosensor and the second for a sentinel carbon sensor.

2.3.2. Biosensors' design and calibration

The GOx-based biosensors (Pt/(PEI+BSA-GOx)$_5$/PU) for glucose absorption detection (Fig. 3A) were prepared 24 h before their use, following a previously described procedure (Rocchitta et al., 2013) with modifications. A Pt/Ir cylinder electrode (1 mm) was connected to a potentiostat (eDAQ Quadstat, e-Corder 410, eDAQ Europe, Poland) and placed in an electrochemical cell containing a 250 mM solution of OPD monomer. The electropolymerization of OPD to poly(*o*-phenylenediamine) was obtained at +700 mV *vs* Ag/AgCl reference electrode for 15 min, and the modified

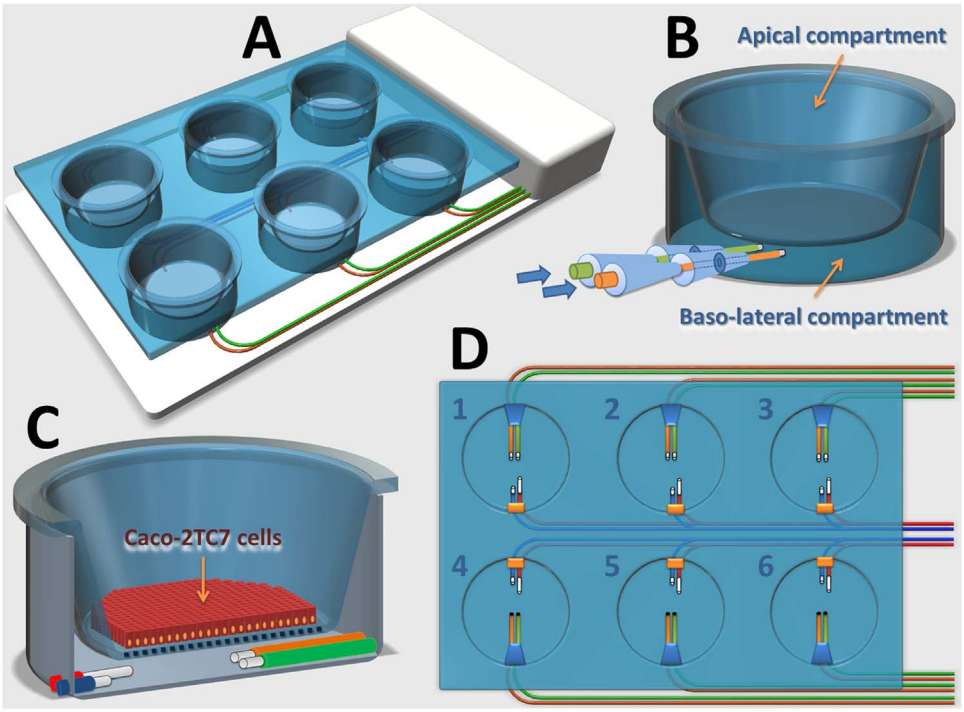

Fig. 1. (A) Schematic drawing of the diagnostic device used in this study. The case including the two potentiostats is integrated with the Corning® 6-wells cell culture plate. (B) Drawing of the lateral access holes for the working electrodes (WEs) of SB1 and SB2. (C) Drawing of the WEs (biosensor = green wire; sentinel sensor = orange wire) aligned in the free space between the bottom of the well and the bottom of the insert containing the Caco-2TC7 cells. (D) Schematic drawing of shared auxiliary (AUX = red wire) and reference (REF = blue wire) electrodes systems, arranged at the bottom of the plate. Ag/AgCl Ref and Pt Aux electrode were positioned in each well. (For interpretation of the references to color in this figure legend, the reader is referred to the web version of this article.)

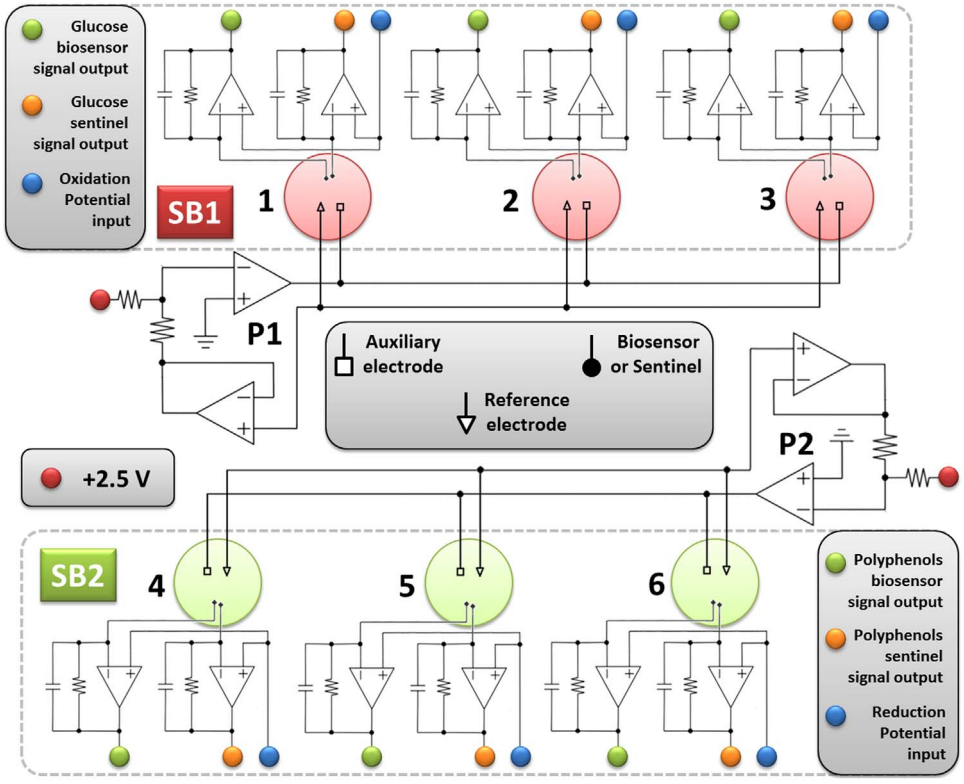

Fig. 2. Schematic drawing of the amperometric module of the diagnostic device and its connections to the digital module (Supplementary data, S-4.1). The module was made using four quad operational amplifiers, twelve feedback resistors and capacitors and few extra components on a dual side PCB. Each sensors/biosensors system (SB1 an SB2) uses a dedicated potentiostat, P1 and P2, which guarantees that reference electrode and auxiliary electrode potentials are fixed to 2.5 V. Each working electrode (biosensor or sentinel) has a dedicated current-to-voltage converter. SB1 was polarized at 3.2 V (+700 mV *vs* Ag/AgCl) while SB2 was polarized at 2.4 V (−100 mV *vs* Ag/AgCl).

Please cite this article as: Antonio, B., et al., Biosensors and Bioelectronics (2016), http://dx.doi.org/10.1016/j.bios.2016.08.007

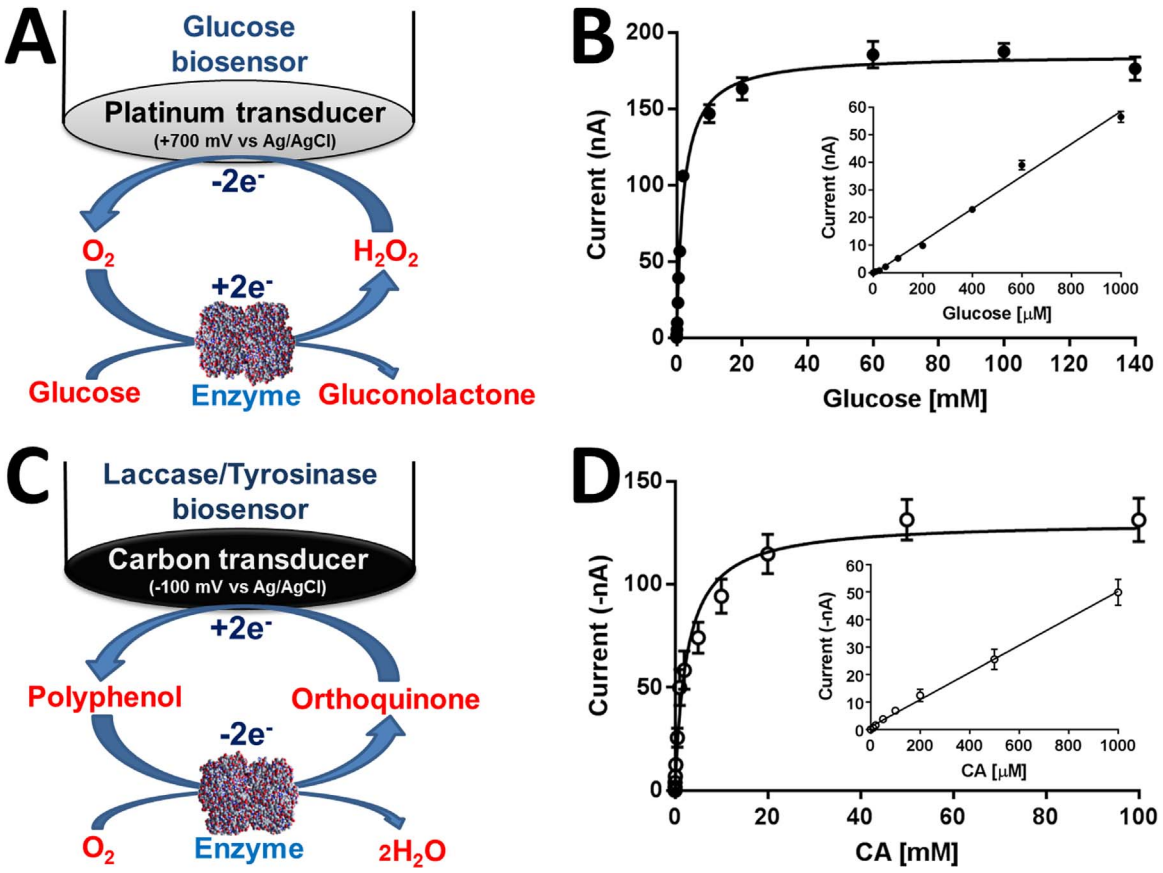

Fig. 3. (A) Schematic representation of GOx-based biosensor used in this study, with the glucose oxidase reaction mechanism and H_2O_2 oxidation on the transducer surface. (B) Michaelis-Menten kinetics of GOx-based biosensor and glucose calibration in the 0–1 mM linear region (inset). (C) Schematic representation of Lac/Tyr-based biosensor used in this study, with the polyphenols oxidation reaction mechanism and orthoquinones reduction on the transducer surface. (D) Michaelis-Menten kinetics of Lac/Tyr-based biosensor and chlorogenic acid calibration in the 0–1 mM linear region (inset).

transducer was stored at 4 °C. A layer of PEI, an enzyme stabilizer, was deposited on the sensor surface by dip-evaporation from a 1% PEI aqueous solution, then BSA and GOx were loaded on the sensor surface by dip-evaporation from a 25 μL of a 10% BSA solution containing 200 U of enzyme. This procedure was repeated five times. A final layer of polyurethane was applied on the biosensor surface by a quick dip in a 1% PU solution. The sentinel Pt sensor (Pt/$(PEI+BSA)_5$/PU) differed from the biosensor only for the absence of GOx. It was used to record the oxidation signal of the interferents present in the matrix that pass through the poly(*o*-phenylenediamine) permselective film; this signal was subtracted from the current recorded by the corresponding biosensor.

The Lac/Tyr-based biosensors (C/$(BSA\text{-}Lac/Tyr)_2$/PU) for polyphenols absorption detection (Fig. 3C) were prepared 24 h before their use, modifying a previous design (Barberis et al., 2010). The transductors were 5 mm carbon rods with a 300 μm diameter (commercial 2H Staedtler graphite pencil leads). The rods were previously insulated with epoxy resin, then inserted in a 15 mm polyethylene tube (diameter =0.58 mm) and dried in oven at 55 °C overnight. The electrical connection between the rods and a length of insulated copper wire was assured by means of graphite loaded epoxy-resin (Bazzu et al., 2009). A transducer circular active surface of 0.071 mm^2 was obtained by drilling the rods with a high speed drill equipped with an aluminum oxide grinding wheel. The enzymes were loaded by deposition of 1+1 μL of a Lac/Tyr solution made of 10 U/mL Tyr and 0.04 U/mL Lac. An entrapment layer of PU was obtained by a quick-dip in a 1% PU solution which dried at room temperature for 30 min. The sentinel carbon sensor (C/$(BSA)_2$/PU) differed from the biosensor only for the absence of the enzymes Lac and Tyr. It did not give any response to chlorogenic acid exposure, and was used to record the signal corresponding to quinones originated by polyphenols autoxidation; this signal was subtracted from the current recorded by the corresponding biosensor.

All the calibrations were performed at 37 °C by constant potential amperometry, using the above mentioned Quadstat, in order to evaluate apparent Michaelis-Menten parameters (V_{MAX} and K_M) and linear region slope (LRS), where the GOx- and the Lac/Tyr-based biosensors exhibit a linear response to glucose or chlorogenic acid (CA) concentrations respectively. Chlorogenic acid was selected as standard calibrator for Lac/Tyr-based biosensors since it is well represented both in blueberry and pomegranate juices (Barberis et al., 2015; Fischer et al., 2011) and the signals recorded in the basolateral compartment were expressed as chlorogenic acid equivalents (CAE) to allow the comparison between the absorption of polyphenols present in the two juices.

The GOx-based biosensors were calibrated fixing the applied potential for H_2O_2oxidation at +700 mV *vs* Ag/AgCl. In this particular design, the oxidation potential was selected to be the high as possible for good H_2O_2 sensitivity and concurrently ensure a good immunity against interferences (O'Neill et al., 2004; Kirwan et al., 2007).

After a stable baseline was reached, a 12-point calibration was made by adding known amounts of glucose ranging from 0.1 to 140 mM. After the last injection, the biosensors were washed with bidistilled water and immersed in fresh PBS solution to be re-stabilized for samples' glucose detection. The Lac/Tyr-based biosensors were immersed in 20 mL of PBS (pH=7.4) and a fixed potential of −100 mV *vs* Ag/AgCl was applied (Supplementary data, S4). When stabile baselines were reached, the biosensors

were calibrated by adding known volumes of 1 M and 100 mM standard solutions of CA, in a concentration range from 0 up to 100 mM.

2.3.3. The apical compartment

The apical compartment was represented by a cell culture insert placed in each of the six wells (Fig. 1C). In these inserts Caco-2TC7 cells were prepared as reported in D'Antuono et al. (2015) with some modifications. The complete procedure was provided in Supplementary data (S5).

2.4. Experimental design

Preliminary experiments were performed in order to evaluate the kinetic of glucose diffusion through the tracked-etched membrane of the inserts without Caco-2TC7 cells after the addition of 0.5, 1 or 2 mM glucose in the apical compartment.

Preliminary toxicity experiments were carried out on the basis of previous protocol (Minervini et al., 2014), in order to assess the highest non-cytotoxic dilution of pomegranate and blueberry juices, by using the MTT test. Transepithelial electrical resistance (TEER) determination was used to measure the integrity of cell monolayers. The complete procedures were provided in Supplementary data (S5). The real-time telemetric monitoring of glucose and phenols absorption by Caco-2TC7 human intestinal cell culture was assessed by the previously described diagnostic device. Three wells were connected to the potentiostat A and used, with SB1, for glucose detection. Three wells were connected to the potentiostat B and used, with SB2, for polyphenols detection. The basolateral compartments were all filled with 3 mL of PBS, then inserts with the Caco-2TC7 cells were gently added in each well.

All the experiments were carried out for 2 h in order to simulate a postprandial phase, and the device was put inside a oven to ensure a constant 37 °C temperature. Glucose and polyphenols relative currents were recorded in the basolateral compartment, in the absence and in the presence of the inhibitors phloridzin (inhibitor of SGLT1 glucose transporter), phloretin-2 O-xyloglucoside (inhibitor of GLUT2 glucose transporter) and of blueberry or pomegranate juices.

In order to have four treatments the following solutions were added to apical compartment:

1. *Control* samples: 2 mL of 1 mM standard glucose solution (as suggested by Manzano et al. (2010));
2. Samples with *Inhibitors*: 2 final milliliters of PBS solution containing 0.6 mM phloridzin, 0.2 mM phloretin and 1 mM standard glucose. Inhibitors were added 10 min before glucose addition;
3. Samples with *Blueberry juice*: 2 mL of PBS solution containing diluted (1:2.5) blueberry juice and 1 mM standard glucose;
4. Samples with *Pomegranate juice*: 2 mL of PBS solution containing diluted (1:10) pomegranate juice and 1 mM standard glucose.

Both juices were added 10 min before the glucose solution addition. Almost three independent experiments were carried out for each thesis.

2.5. Statistical analysis

Glucose and phenol phytochemicals currents were expressed in nanoamperes (nA) and given as mean ± standard error of the mean of absolute oxidation (for glucose) or reduction (for phenols) currents (nA) or baseline-subtracted currents (ΔnA). Glucose content was expressed as molarity to be comparable with reference methods. Phenols content was expressed as chlorogenic acid equivalents (CAE).

Statistical analysis was performed by GraphPad Prism 5.02 for Windows software (GraphPad Software, Inc., La Jolla, CA 92037, USA). Analysis of variance (one-way ANOVA) was performed to compare results obtained with different analytical methods, using a unifactorial complete randomized block design. Mean comparisons were calculated by Fisher's least significant difference test at $P \leq 0.05$.

3. Results

3.1. Preliminary characterization of biosensors

As described before, the biosensors and the sentinel sensors of SB1 and SB2 differed only for the presence or the absence of GOx and Lac/Tyr respectively. The influence of PEI, BSA and PU on Pt and C electrodes were previously investigated (Rocchitta et al., 2013; Barberis et al., 2015). *In-vitro* calibrations of biosensors were carried out in fresh PBS at 37 °C (Fig. 3).

SB1 recorded currents relative to H_2O_2, originated from the enzymatic glucose oxidation, on the transductor surface at an applied potential of +700 mV *vs* Ag/AgCl (Fig. 3A). The GOX-based biosensors calibration data fitted with the Michaelis-Menten equation ($r^2=0.9873$, n =6) with $V_{max}=185.4 \pm 5.2$ nA and $K_m=2.096 \pm 0.6$ mM (Fig. 3B). The response to low concentrations of glucose (0 – 1 mM) revealed excellent linearity ($r^2=0.9928$, n =6) and a LRS $=0.059 \pm 0.0019$ nA*μM^{-1}.

SB2 recorded currents of quinones resulting from polyphenols oxidation by Lac and Tyr and later reduced on the transductor surface at −100 mV *vs* Ag/AgCl (Fig. 3C). Lac/Tyr-based biosensors also displayed a Michaelis-Menten kinetics (Fig. 3D) with $V_{max}=130.4 \pm 8.9$ nA and $K_m=2.572 \pm 0.9$ mM, and an excellent response to low concentrations of chlorogenic acid (0–1 mM) with $r^2=0.9973$ (n =6) and LRS $=0.049 \pm 0.001$ nA*μM^{-1}.

The limit of detection of the biosensors (LOD =3.3 σ/S), where σ is the standard deviation of background noise of the biosensor and *S* is the slope of the linear region of the calibration curve were 0.85 ± 0.07 μM and 1.59 ± 0.09 μM for GOX-based biosensors and Lac/Tyr-based biosensors respectively. The corresponding limits of quantification (LOQ =3*LOD) were 2.55 ± 0.21 μM and 4.77 ± 0.27 μM.

3.2. Kinetic of glucose diffusion in absence of cellular monolayer

The results indicated that, in absence of a cellular monolayer the glucose diffusion from apical to basolateral compartment was dose-dependent (Fig. 4). The curves of recorded currents were smooth and followed non-linear hyperbolic trends according to the equation $Y = Bmax*X/(Kd+X)$ where the glucose concentration Y is zero initially, and increases to a maximum plateau value Bmax, and *Kd* is the time X needed to achieve a half of *Bmax*. In this work, curves are characterized by growing values of *Bmax* (199.5 μM, 394.8 μM and 794.8 μM) and by decreasing value of *Kd* (165.3 min, 95.16 min and 61.68 min) for 0.5 mM, 1 mM and 2 mM of glucose respectively. The experiment lasted 2 h while a linear trend was observed for 30 min from the glucose injection with $r^2=0.995$, 0.997 and 0.998 for 0.5 mM (LRS $=0.119 \pm 0.0002$ μM*min^{-1}), 1 mM (LRS $=0.283 \pm 0.0003$ μM*min^{-1}) and 2 mM (LRS $=1.03 \pm 0.002$ μM*min^{-1}) of glucose respectively (Fig. 4 inset).

3.3. Kinetic of glucose $CaCo_2$absorption in presence and in absence of inhibitors

Glucose absorption, from apical to basolateral compartment through the Caco-2TC7 monolayer, was detected, in absence and in

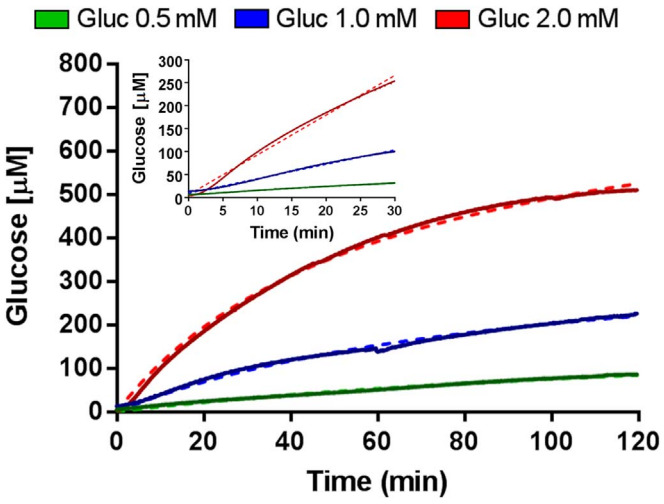

Fig. 4. Kinetics of 0.5 mM, 1 mM and 2 mM glucose passive diffusion through the tracked-etched membrane of the inserts, in a 2 h time range and in the first 30 min of the experiment (inset).

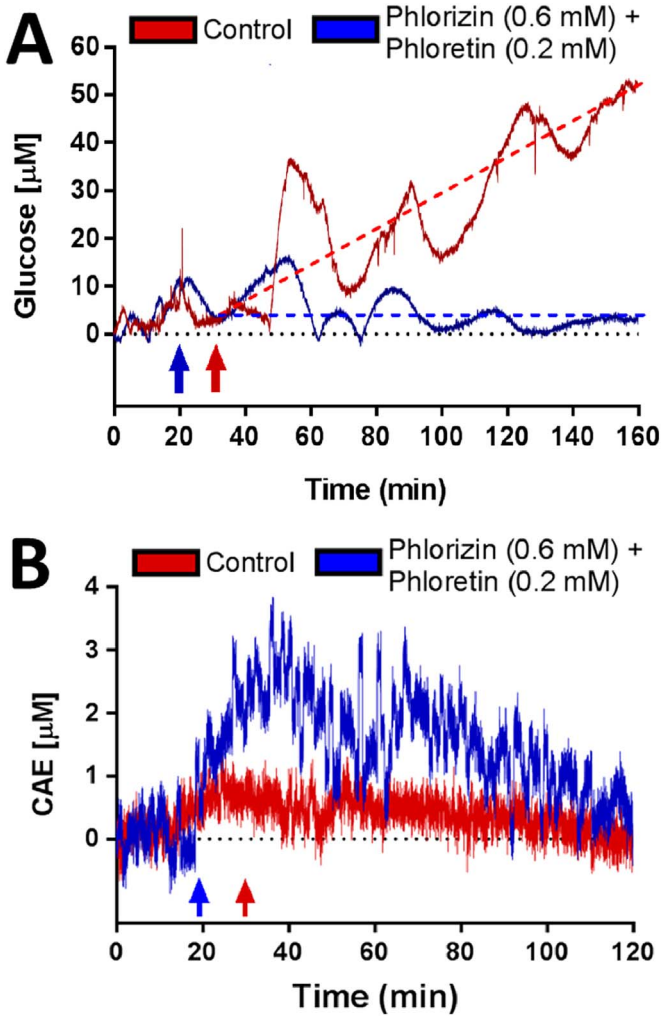

Fig. 5. (A) Kinetics of 1 mM glucose active transporttrough the Caco-2-TC7 cells monolayerin the absence and in the presence of glucose transport inhibitors phlorizin and phloretin. (B) Kinetics of inhibitors active transporttrough the Caco-2-TC7 cells monolayer in the presence of 1 mM glucose.

presence of glucose transporters inhibitors (Fig. 5A). In presence of the cell monolayer a delay of glucose absorption after its addition was observed indicating an active transport rather than a diffusion. In the *Control* a peak of about 40 μM was recorded 20 min after the glucose administration, and then the transport from the apical to the basolateral compartment continued irregularly but with gradually decreasing fluctuations. Even though the phenomenon cannot be ascribed to a particular mathematical model (due to the above-mentioned fluctuations), a linear trend can be hypothesized with a slope of 0.3668 ± 0.001 μM/min (dotted line in Fig. 5A). A similar irregular trend was also observed in the presence of phloridzin and phloretin two recognized glucose transporters inhibitors (Zheng et al., 2012). A quite horizontal trend (slope $=0.0094 \pm 0.0006$ μM/min) was observed. The results obtained with glucose biosensor, at the end of the experiment, were compared with HPLC reference method. In particular, the amounts of glucose recovered were 51.03 ± 3.47 μM *vs* 47.7 ± 4.01 μM in the control and 3.67 ± 2.4 μM *vs* 5.15 ± 2.9 μM with the inhibitors, for SB1 and HPLC analysis, respectively. All considered, the glucose bioavailability in the *Control* was 5.1% for biosensor determination and 4.8% by HPLC determination; instead, in the presence of inhibitors, the glucose bioavailability decreased of about 10 times for both determinations. The kinetic of inhibitors transport from apical to basolateral compartment, in the presence of 1 mM glucose, was also monitored by SB2 (Fig. 5B). Phloretin and phloridzin were minimally transported in the basolateral compartment. Their absorption was characterized by two main waves during the first 60 min of the experiment, and then the signal progressively decreased. Results obtained using HPLC-DAD analysis at the end of experiments showed a low amount of inhibitors absorption in the basolateral side, 0.80 μM for phloridzin and 0.98 μM for phloretin, corresponding to 0.13% and 0.49% of bioavailability, respectively.

3.4. The case study: kinetic of glucose and phenols active transport in the presence of pomegranate and blueberry juices

The hypoglycemic potential of blueberry and pomegranate juices was also studied. The juices were characterized by 1.3 g*100 mL^{-1} and 9.8 g*100 mL^{-1} glucose and 24.3 mg*100 mL^{-1} (33% anthocyanins) and 15.3 mg*100 mL^{-1} (52.8% anthocyanins) polyphenols, respectively. On the basis of the preliminary determination of non-cytotoxic blueberry and pomegranate juices, 1:2.5 and 1:10 dilutions for blueberry and pomegranate respectively, were added in the apical compartment before the glucose addition.

Results showed a quite linear increase of glucose absorption, even if with some fluctuations, in the presence of blueberry or pomegranate juices ($r^2=0.9143$ and $r^2=0.9691$ respectively) (Fig. 6A). The slopes of the dotted lines indicated that glucose was absorbed with different velocity (0.413 ± 0.0015 and 3.04 ± 0.006 μM*min^{-1}). Data recorded by SB1 at the end of the experiment were 53.2 ± 8.4 μM and 387.5 ± 14 μM for blueberry and pomegranate, respectively, showing that, in the presence of pomegranate juice a higher amount of glucose was transported through the Caco-2TC7 monolayer in the basolateral side (8‰) respect to the blueberry juice (1.7‰).

The curves of polyphenols absorption (Fig. 6B) followed trends similar to those previously observed for phloretin and phloridzin. An increasing of polyphenols absorption was recorded by SB2 during the first 50 min for blueberry and pomegranate, then a constant decreasing occurred, reaching values very closed to the LOD at the end of the experiment. A higher amount of polyphenols was recorded for pomegranate juice in the basolateral side.

Please cite this article as: Antonio, B., et al., Biosensors and Bioelectronics (2016), http://dx.doi.org/10.1016/j.bios.2016.08.007

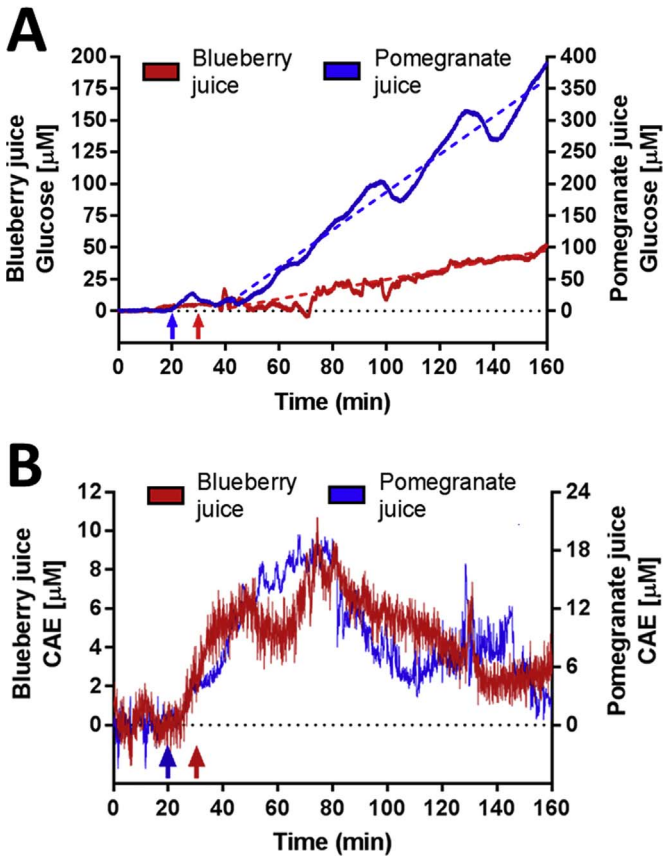

Fig. 6. (A) Kinetics of glucose active transporttrough the Caco-2-TC7 cells monolayer in the presence of blueberry and pomegranate juice. (B) Kinetics of blueberry's and pomegranate's polyphenols active transporttrough the Caco-2-TC7 cells monolayer.

4. Discussion

The integrated device proposed in this paper combines different analytical systems with the purpose to study the kinetic of glucose absorption in the presence of various phytochemicals. The originality of the system is testified to the absence in the literature, as far as we know, of similar device. At the same time the reliability is ensured, since sensor/biosensors systems were successfully employed to detect glucose (Wu et al., 2015; Arango Gutierrez et al., 2013; Yoo and Lee, 2010) and phenol compounds (Rodríguez-Delgado et al., 2015; Carralero Sanz et al., 2005; Gomes et al., 2004), while Caco-2TC7 cell-based model have been already used to assess the reduction of glucose transport by polyphenols (Farrell et al., 2013; Manzano and Williamson, 2010).

The device showed that, in the absence of a cell monolayer, SB1 registered a dose-dependent glucose diffusion. In the presence of Caco-2TC7 cells, the glucose transport to the basolateral compartment was not immediate and got slower following a quite linear trend characterized by fluctuations. The maximum glucose level was recorded after 20 min. Five times higher glucose level was found by Manzano and Williamson (2010) after 30 min of radiolabel glucose (1 mM) exposure of Caco2 cells seeded on polycarbonate transwell insert. These results are partially comparable with our findings because of different cell line used (parental Caco2 line *vs* TC7 clone), type of insert (polycarbonate *vs* PET) and the glucose quantification (scintillation counting of radiolabel glucose *vs* sensor/biosensor system). Phloretin and phloridzin strongly affected the glucose absorption, showing their recognized inhibitory effect (Zheng et al., 2012). The mechanisms of glucose absorption in intestinal cell lines are widely studied (El-Zein et al., 2015; Zheng et al., 2012) as far as the interaction of the two inhibitors with SGLT1 and GLUT2 transporters (Farrell et al., 2013; Zheng et al., 2012; Manzano and Williamson, 2010; Drozdowski and Thomson, 2006). Our results, obtained with both methods applied in this study, are in agreement with Scalbert et al. (2002). The Authors indicated that phloretin and phloridzin were only minimally transported in the basolateral compartment according to the fact that their activity was performed principally inside the cells. The lower absorption of phloretin and phloridzin was also in agreement with the poor polyphenols bioavailability as reported by others authors (D'Antuono et al., 2015; Teng et al., 2012).

For the application of this device, interferences in the glucose and phenols detection have also been taken into consideration; H_2O_2 not originated by the glucose oxidase, for example from polyphenols autoxidation (Akagawa et al., 2003), could represent interference when quantifying the amount of glucose in the basolateral compartment. The sentinel Pt sensor was used to record the oxidation signal of H_2O_2 of different origin and its signal was subtracted from the current recorded by the corresponding biosensor. On the other hand, according to its mechanism of action, SB2 should reduce only quinones resulting from polyphenols oxidized by Lac and Tyr, but it is also able to reduce quinones originated by polyphenols autoxidation. During our experiments, the carbon sentinel sensors, which did not give any response to chlorogenic acid exposure, recorded a current of few nanoamperes. We hypothesized that this signal corresponds to quinones originated by polyphenols autoxidation; for these reasons, it appears essential to maintain the sentinel sensors and to subtract their signals from the signals of the corresponding biosensors.

In this work an application of the device was provided and the hypoglycemic potential of blueberry and pomegranate juices was also studied. The outcome of our experiments indicated that, the glucose absorption was higher in the presence of pomegranate juice than blueberry juice. Previous investigations were carried out on the hypoglycemic activity of polyphenols of blueberry (Grace et al., 2009; McDougall and Stewart, 2005) and pomegranate (Kaur et al., 2014; Parmar and Kar, 2007), suggesting that this role is principally performed by anthocyanins. In particular, concerning blueberry, its hypoglycemic effect was studies in *in vivo* models and was related to inhibitory effect of anthocyanins on alpha-glucosidase activity (McDougall and Stewart, 2005). Other authors (Grace et al., 2009), in *in vivo* diabetic mice, reported the greater hypoglycemic activity of anthocyanin-enriched fraction compared to the parent phenolic rich extract of blueberry, suggesting that the hypoglycemic activity of blueberry can be specifically ascribed to anthocyanins. In our study this different hypoglycemic behavior of the two juices could be also attributed to the different polyphenols composition. In fact, blueberry juice, behind the anthocyanins, is characterized by a higher amount of flavonoids, which showed chemical structure similar to phloretin and phloridzin and could be also responsible to the hypoglycemic effect (Kwon et al., 2007).

Concerning the polyphenols absorption, the quantity of pomegranate polyphenols, recorded by SB2 biosensors, was higher than of blueberry. Considering the high metabolic activity of Caco-2TC7, related to high expression of phase II enzymes, the determination of polyphenols in the basolateral side should be performed by a sensitive and reliable analytical methods capable of measuring polyphenols and their metabolism (Teng et al., 2012). Since the SB2 biosensor was calibrated only with CA, the comparison between results obtained with this biosensor and HPLC analysis was in agreement only for binary mixtures (such as phloridzin and phloretin solution); instead, in the case of complex mixtures (such as the juices) or in the presence of metabolites (that could be generated by the Caco-2TC7 activities), the

biosensor is not able to discriminate among the molecules with high level of complexity.

5. Conclusion

The device was conceived for the on-line *in vitro* assessment of the glucose bioavailability, in absence and in presence of glucose inhibitors. An application of the system was carried out providing the trend of glucose and phenols absorption in presence of blueberry and pomegranate juices. The use of the device can easily be extended to other phytochemicals with presumed hypoglycemic activity. It is our opinion that the object to realize a smart tool to study the effects of a wide variety of phytochemicals on the glucose absorption and to contribute to an effective strategy for managing postprandial hyperglycemia with natural compounds, was achieved.

It is also clear that this system cannot be alternative to the reference methods but that it could be complementary to them. HPLC method, which is expensive and time-consuming, cannot describe trends but it provides accurate bioactive compounds characterization allowing to discriminate among different polyphenols classes. Consequently, the proposed system can be used for a rapid screening of natural compounds that can modulate glucose bioavailability, and only the phytochemicals, with demonstrated hypoglycemic activity, should be further investigated with traditional systems.

Finally, together with the present device we propose an original approach, in support of drug therapy, for a better management or prevention of T2DM. This approach can be easily extended to studies on different diseases by using different cellular models and/or different biosensor systems.

Acknowledgments

The purchase of Multimode Reader Varioskan was funded by Programma Operativo Regionale Puglia FESR 2000–2006 – Risorse liberate – Obiettivo Convergenza, Progetto Reti di Laboratorio “Biodiversità per la valorizzazione e sicurezza delle produzioni alimentari tipiche pugliesi, BioNet-PTP” (Cod. 73).

This work was partially supported by MiEF – CNR, Project “Innovazione e Sviluppo del Mezzogiorno – Conoscenze Integrate per Sostenibilità ed Innovazione del Made in Italy Agroalimentare – Legge n.191/2009”.

Appendix A. Supplementary data

Supplementary data associated with this article can be found in the online version at http://dx.doi.org/10.1016/j.bios.2016.08.007.

References

Akagawa, M., Shigemitsu, T., Suyama, K., 2003. Biosci. Biotechnol. Biochem. 67 (12), 2632–2640.
Apetrei, C., Alessio, P., Constantino, C.J.L., de Saja, J.A., Rodriguez-Mendez, M.L., Pavinatto, F.J., Fernandes, E.G.R., Zucolotto, V., Oliveira Jr, O.N., 2011. Biosens. Bioelectron. 26 (5), 2513–2519.
Arango Gutierrez, E., Mundhada, H., Meier, T., Duefel, H., Bocola, M., Schwaneberg, U., 2013. Biosens. Bioelectron. 50, 84–90.
Artursson, P., Palm, K., Luthman, K., 2012. Adv. Drug Del. Rev. 64 (Supplement), 280–289.
Atkinson, C.J., Nestby, R., Ford, Y.Y., Dodds, P.A.A., 2005. Biofactors 23 (4), 229–234.
Barberis, A., Bazzu, G., Calia, G., Puggioni, G.M.G., Rocchitta, G.G., Migheli, R., Schirra, M., Desole, M.S., Serra, P.A., 2010. Anal. Chem. 82 (12), 5134–5140.
Barberis, A., Spissu, Y., Bazzu, G., Fadda, A., Azara, E., Sanna, D., Schirra, M., Serra, P. A., 2014. Anal. Chem. 86 (17), 8727–8734.
Barberis, A., Spissu, Y., Fadda, A., Azara, E., Bazzu, G., Marceddu, S., Angioni, A., Sanna, D., Schirra, M., Serra, P.A., 2015. Biosens. Bioelectron. 67 (0), 214–223.
Bazzu, G., Puggioni, G.G.M., Dedola, S., Calia, G., Rocchitta, G., Migheli, R., Desole, M. S., Lowry, J.P., O'Neill, R.D., Serra, P.A., 2009. Anal. Chem. 81 (6), 2235–2241.
Carralero Sanz, V., Mena, M.L., González-Cortés, A., Yáñez-Sedeño, P., Pingarrón, J. M., 2005. Anal. Chim. Acta 528 (1), 1–8.
Ceriello, A., Motz, E., 2004. Arterioscler. Thromb. Vasc. Biol. 24 (5), 816–823.
Chacón, M.R., Ceperuelo-Mallafré, V., Maymó-Masip, E., Mateo-Sanz, J.M., Arola, L., Guitiérrez, C., Fernandez-Real, J.M., Ardèvol, A., Simón, I., Vendrell, J., 2009. Cytokine 47 (2), 137–142.
Chu, Y.-F., Chen, Y., Black, R.M., Brown, P.H., Lyle, B.J., Liu, R.H., Ou, B., 2011. Food Chem. 124 (3), 914–920.
Clark, L.C., Lyons, C., 1962. Ann. NY Acad. Sci. 102 (1), 29–45.
D'Antuono, I., Garbetta, A., Linsalata, V., Minervini, F., Cardinali, A., 2015. Food Funct. 6 (4), 1268–1277.
Drozdowski, L., Thomson, A.B., 2006. World J. Gastroenterol. 12 (11), 14.
El-Zein, O., Usta, J., Kreydiyyeh, S.I., 2015. Cell. Physiol. Biochem. 37 (2), 491–500.
Failla, M.L., Chitchumronchokchai, C., Ferruzzi, M.G., Goltz, S.R., Campbell, W.W., 2014. Food Funct. 5 (6), 1101–1112.
Farrell, T.L., Ellam, S.L., Forrelli, T., Williamson, G., 2013. Biofactors 39 (4), 448–456.
Fischer, U.A., Carle, R., Kammerer, D.R., 2011. Food Chem. 127 (2), 807–821.
Gomes, S.A.S.S., Nogueira, J.M.F., Rebelo, M.J.F., 2004. Biosens. Bioelectron. 20 (6), 1211–1216.
Grace, M.H., Ribnicky, D.M., Kuhn, P., Poulev, A., Logendra, S., Yousef, G.G., Raskin, I., Lila, M.A., 2009. Phytomedicine 16 (5), 406–415.
Hanhineva, K., Törrönen, R., Bondia-Pons, I., Pekkinen, J., Kolehmainen, M., Mykkänen, H., Poutanen, K., 2010. Int. J. Mol. Sci. 11 (4), 1365.
Johnston, K., Sharp, P., Clifford, M., Morgan, L., 2005. FEBS Lett. 579 (7), 1653–1657.
Kaur, C., Pal, R.K., Kar, A., Gadi, C., Sen, S., Kumar, P., Chandra, R., Jaiswal, S., Khan, I., 2014. J. Food Biochem. 38 (4), 397–406.
Kirwan, S.M., Rocchitta, G., McMahon, C., Craig, J.D., Killoran, S.J., O'Brien, K.B., Serra, P.A., Lowry, J.P., O'Neill, R.D., 2007. Sensors 7, 420–437.
Kwon, O., Eck, P., Chen, S., Corpe, C.P., Lee, J.-H., Kruhlak, M., Levine, M., 2007. FASEB J. 21 (2), 366–377.
Manzano, S., Williamson, G., 2010. Mol. Nutr. Food Res. 54 (12), 1773–1780.
McDougall, G.J., Stewart, D., 2005. Biofactors 23 (4), 189–195.
Minervini, F., Garbetta, A., D'antuono, I., Cardinali, A., Martino, N.A., Debellis, L., Visconti, A., 2014. Arch. Environ. Contam. Toxicol. 67 (1), 9.
Shihabudeen, Mohamed Sham, Hansi Priscilla, H., Thirumurugan, K, D., 2011. Nutr. Metab. 8 (1), 1–11.
O'Neill, R.D., Chang, S., Lowry, J.P., McNeil, C.J., 2004. Biosens. Bioelectron. 19 (1), 1521–1528.
Parmar, H.S., Kar, A., 2007. Biofactors 31 (1), 17–24.
Rechner, A.R., Kuhnle, G., Bremner, P., Hubbard, G.P., Moore, K.P., Rice-Evans, C.A., 2002. Free Radic. Biol. Med. 33 (2), 220–235.
Rocchitta, G., Migheli, R., Dedola, S., Calia, G., Desole, M.S., Miele, E., Lowry, J.P., O'Neill, R.D., Serra, P.A., 2007. Sens. Actuators B: Chem. 126 (2), 700–709.
Rocchitta, G., Secchi, O., Alvau, M.D., Farina, D., Bazzu, G., Calia, G., Migheli, R., Desole, M.S., O'Neill, R.D., Serra, P.A., 2013. Anal. Chem. 85 (21), 10282–10288.
Rodríguez-Delgado, M.M., Alemán-Nava, G.S., Rodríguez-Delgado, J.M., Dieck-Assad, G., Martínez-Chapa, S.O., Barceló, D., Parra, R., 2015. TrAC Trends Anal. Chem. 74, 21–45.
Scalbert, A., Morand, C., Manach, C., Rémésy, C., 2002. Biomed. Pharmacother. 56 (6), 276–282.
Serra, P.A., Rocchitta, G., Bazzu, G., Manca, A., Puggioni, G.M., Lowry, J.P., O'Neill, R. D., 2007. Sens. Actuators B: Chem. 122 (1), 118–126.
Teng, Z., Yuan, C., Zhang, F., Huan, M., Cao, W., Li, K., Yang, J., Cao, D., Zhou, S., Mei, Q., 2012. PLoS One 7 (1), e29647.
Wright, E. Jr., Scism-Bacon, B.L., Glass, L.C., 2006. Int J Clin Pract. 60 (3), 308–314.
Wu, C., Sun, H., Li, Y., Liu, X., Du, X., Wang, X., Xu, P., 2015. Biosens. Bioelectron. 66, 350–355.
Yoo, E.-H., Lee, S.-Y., 2010. Sensors 10 (5), 4558.
Zheng, Y., Scow, J.S., Duenes, J.A., Sarr, M.G., 2012. Surgery 151 (1), 13–25.